CHAPTER 3.

Broad-Scale Patterns of Forest Fire Occurrence across the 50 United States and the Caribbean Territories, 2018

Kevin M. Potter

INTRODUCTION

As a pervasive disturbance agent operating at many spatial and temporal scales, wildland fire is a key abiotic factor affecting forest health both positively and negatively. In some ecosystems, for example, wildland fires have been essential for regulating processes that maintain forest health (Lundquist and others 2011). Wildland fire is an important ecological mechanism that shapes the distributions of species, maintains the structure and function of fire-prone communities, and acts as a significant evolutionary force (Bond and Keeley 2005). At the same time, wildland fires have created forest health (i.e., sustainability) problems in some ecosystems (Edmonds and others 2011).

Current fire regimes on more than half of the forested area in the conterminous United States have been moderately or significantly altered from historical regimes (Barbour and others 1999), potentially altering key ecosystem components such as species composition, structural stage, stand age, canopy closure, and fuel loadings (Schmidt and others 2002). Fires in some regions and ecosystems have become larger, more intense, and more damaging because of the accumulation of fuels as a result of prolonged fire suppression (Pyne 2010). In some regions, plant communities have experienced or are undergoing rapid compositional and structural changes as a result of fire suppression (Nowacki and Abrams 2008). Additionally, changes in fire intensity and recurrence could result in decreased forest resilience and persistence (Lundquist and others 2011), and fire regimes altered by global climate change could cause large-scale shifts in vegetation spatial patterns (McKenzie and others 1996).

At the same time, large wildland fires also can have long-lasting social and economic consequences, which include the loss of human life and property, smoke-related human health impacts, and the economic cost and dangers of fighting the fires themselves (Gill and others 2013, Richardson and others 2012).

This chapter presents analyses of daily satellite-based fire occurrence data that map and quantify the locations and intensities of fire occurrences spatially across the conterminous United States, Alaska, Hawaii, and the Caribbean territories in 2018. It also compares 2018 fire occurrences, within a geographic context, to all the recent years for which such data are available. Quantifying and monitoring such large-scale patterns of fire occurrence across the United States can help improve our understanding of the ecological and economic impacts of fire as well as the appropriate management and prescribed use of fire. Specifically, large-scale assessments of fire occurrence can help identify areas where specific management activities may be needed, or where research into the ecological and socioeconomic impacts of fires may be required. Additionally, given the potential for climate change and shifting species distributions to alter historic fire regimes, quantifying the location and frequency

of forest fire occurrences across the United States can help us to better understand emerging spatiotemporal patterns of fire occurrence.

METHODS

Data

Annual monitoring and reporting of active wildland fire events using the Moderate Resolution Imaging Spectroradiometer (MODIS) Active Fire Detections for the United States database (USDA Forest Service 2019) allow analysts to spatially display and summarize fire occurrences across broad geographic regions (Coulston and others 2005; Potter 2012a, 2012b, 2013a, 2013b, 2014, 2015a, 2015b, 2016, 2017, 2018, 2019). A fire occurrence is defined as one daily satellite detection of wildland fire in a 1-km pixel, with multiple fire occurrences possible on a pixel across multiple days resulting from a single wildland fire that lasts more than 1 day. The data are derived using the MODIS Rapid Response System (Justice and others 2002, 2011) to extract fire location and intensity information from the thermal infrared bands of imagery collected daily by two satellites at a resolution of 1 km, with the center of a pixel recorded as a fire occurrence (USDA Forest Service 2019). The Terra and Aqua satellites' MODIS sensors identify the presence of a fire at the time of image collection, with Terra observations collected in the morning and Aqua observations collected in the afternoon. The resulting fire occurrence data represent only whether a fire was active because the MODIS data bands may not differentiate between a hot fire in a relatively small area (0.01 km^2, for example) and a cooler fire over a larger area (1 km^2, for example) if the foreground to background temperature contrast is not sufficiently high. The MODIS Active Fire database does well at capturing large fires during cloud-free conditions but may underrepresent rapidly burning, small, and low-intensity fires, as well as fires in areas with frequent cloud cover (Hawbaker and others 2008). For large-scale assessments, the dataset represents a good alternative to the use of information on ignition points, which may be preferable but can be difficult to obtain or may not exist (Tonini and others 2009). For more information about the performance of this product, see Justice and others (2011). The fire occurrence data additionally do not differentiate fires intentionally set for management purposes (controlled burns), which are common in some parts of the United States, particularly in the South.

It is important to underscore that estimates of burned area and calculations of MODIS-detected fire occurrences are two different metrics for quantifying fire activity within a given year. Most importantly, the MODIS data contain both spatial and temporal components because persistent fire will be detected repeatedly over several days on a given 1-km pixel. In other words, a location can be counted as having a fire occurrence multiple times, once for each day a fire is detected at the location. Analyses of the MODIS-detected fire occurrences, therefore, measure the total number of daily

1-km pixels with fire during a year, as opposed to quantifying only the area on which fire occurred at some point during the course of the year. A fire detected on a single pixel on every day of the year would be equivalent to 365 fire occurrences.

It is worth noting that the Terra and Aqua satellites, which carry the MODIS sensors, were launched in 1999 and 2002, respectively, and will eventually be decommissioned. An alternative fire occurrence data source is the Visible Infrared Imaging Radiometer Suite (VIIRS) sensor on board the Suomi National Polar-orbiting Partnership (Suomi NPP) weather satellite. The transition to this new data source will require a comparison of fire occurrence detections between it and MODIS. This is because VIIRS data are available from 2014 onward, but it will be important for assessments of fire occurrence trends to be able to analyze as long a window of time as possible (i.e., from the beginning of MODIS data availability). Additionally, Landsat 8 fire detection data are available at 30-m resolution from 2015 to present, although some issues may affect the completeness of the data (USDA Forest Service 2019).

Analyses

These MODIS products for 2018, and for the 17 preceding full years of data, were processed in ArcMap® (ESRI 2015) to determine forest fire occurrence density (that is, the number of fire occurrences per 100 km^2 [10 000 ha] of tree canopy coverage area) for each ecoregion section in the conterminous United States (Cleland and others 2007), for ecoregions on each of the major islands of Hawaii (see ch. 1 of this report), and for the islands of the Caribbean territories of Puerto Rico and the U.S. Virgin Islands. For the current analyses, the forest fire occurrence density metrics for the conterminous 48 States, Hawaii, and the Caribbean territories (the number of fire occurrences per 100 km^2 of tree canopy cover area) were calculated after screening out wildland fires that did not intersect with tree canopy data. The tree canopy data had been resampled to 240 m from a 30-m raster dataset that estimates percent tree canopy cover (from 0 to 100 percent) for each grid cell; this dataset was generated from the 2011 National Land Cover Database (NLCD) (Homer and others 2015) through a cooperative project between the Multi-Resolution Land Characteristics Consortium and the U.S. Department of Agriculture Forest Service, Geospatial Technology and Applications Center (GTAC) (Coulston and others 2012). For our purposes, we treated any cell with >0 percent tree canopy cover as forest. Comparable tree canopy cover data were not available for Alaska, so we instead created a 240-m-resolution layer of forest and shrub cover from the 2011 NLCD. The MODIS fire occurrence detection data were then intersected with this layer and with ecoregion sections for the State (Spencer and others 2002) to calculate the number of fire occurrences per 100 km^2 of forest and shrub cover within each ecoregion section in Alaska. In previous Forest Health Monitoring national reports, the number of fire occurrences

per 100 km^2 of forest was determined for the conterminous States, Alaska, and Hawaii using a forest cover mask derived from MODIS imagery by the Forest Service GTAC (USDA Forest Service 2008).

The total numbers of forest fire occurrences were also determined separately for the conterminous States, Alaska, Hawaii, and the Caribbean territories after clipping the MODIS fire occurrences by the canopy cover or tree and shrub cover data.

The fire occurrence density value for each of the ecoregions of the States and for the Caribbean islands in 2018 was then compared with the mean fire density values for the first 17 full years of MODIS Active Fire data collection (2001–2017). Specifically, the difference of the 2018 value and the previous 17-year mean for an ecoregion was divided by the standard deviation across the previous 17-year period, assuming a normal distribution of fire density over time in the ecoregion. The result for each ecoregion was a standardized *z*-score, which is a dimensionless quantity describing the degree to which the fire occurrence density in the ecoregion in 2018 was higher, lower, or the same relative to all the previous years for which data have been collected, accounting for the variability in the previous years. The *z*-score is the number of standard deviations between the observation and the mean of the historic observations in the previous years. Approximately 68 percent of observations would be expected within one standard deviation of the mean, and 95 percent within two standard deviations. Near-normal conditions are classified as those within a single standard deviation of the mean, although such a threshold is somewhat arbitrary. Conditions between about one and two standard deviations of the mean are moderately different from mean conditions but are not significantly different statistically. Those outside about two standard deviations would be considered statistically greater than or less than the long-term mean (at $p < 0.025$ at each tail of the distribution).

Additionally, we used the Spatial Association of Scalable Hexagons (SASH) analytical approach to identify forested areas in the conterminous United States with higher-than-expected fire occurrence density in 2018. This method identifies locations where ecological phenomena occur at greater or lower occurrences than expected by random chance and is based on a sampling frame optimized for spatial neighborhood analysis, adjustable to the appropriate spatial resolution, and applicable to multiple data types (Potter and others 2016). Specifically, it consists of dividing an analysis area into scalable equal-area hexagonal cells within which data are aggregated, followed by identifying statistically significant geographic clusters of hexagonal cells within which mean values are greater or less than those expected by chance. To identify these clusters, we employed a Getis-Ord G_i^* hot spot analysis (Getis and Ord 1992) in ArcMap® 10.3 (ESRI 2015).

The spatial units of analysis were 9,810 hexagonal cells, each approximately 834 km^2 in area, generated in a lattice across the

conterminous United States using intensification of the Environmental Monitoring and Assessment Program (EMAP) North American hexagon coordinates (White and others 1992). These coordinates are the foundation of a sampling frame in which a hexagonal lattice was projected onto the conterminous United States by centering a large base hexagon over the region (Reams and others 2005, White and others 1992). The hexagons are compact and uniform in their distance to the centroids of neighboring hexagons, meaning that a hexagonal lattice has a higher degree of isotropy (uniformity in all directions) than does a square grid (Shima and others 2010). These are convenient and highly useful attributes for spatial neighborhood analyses. These scalable hexagons also are independent of geopolitical and ecological boundaries, avoiding the possibility of different sample units (such as counties, States, or watersheds) encompassing vastly different areas (Potter and others 2016). We selected hexagons 834 km^2 in area because this is a manageable size for making monitoring and management decisions in analyses across the conterminous United States (Potter and others 2016).

Fire occurrence density values for each hexagon were quantified as the number of forest fire occurrences per 100 km^2 of tree canopy cover area within the hexagon. The Getis-Ord G_i^* statistic was used to identify clusters of hexagonal cells with fire occurrence density values higher than expected by chance. This statistic allows for the decomposition of a global measure of spatial association into its contributing factors, by location, and is therefore particularly suitable for detecting outlier assemblages of similar conditions in a dataset, such as when spatial clustering is concentrated in one subregion of the data (Anselin 1992).

Briefly, G_i^* sums the differences between the mean values in a local sample, determined in this case by a moving window of each hexagon and its 18 first- and second-order neighbors (the 6 adjacent hexagons and the 12 additional hexagons contiguous to those 6) and the global mean of the 9,644 hexagonal cells with tree canopy cover (of the total 9,810) in the conterminous United States. As described in Laffan (2006), it is calculated as

$$G_i^*(d) = \frac{\sum_j w_{ij}(d)x_j - W_i^*\bar{x}^*}{s^*\sqrt{\frac{(ns_{1i}^*) - W_i^{*2}}{n-1}}}$$

where

G_i^* = the local clustering statistic (in this case, for the target hexagon)

i = the center of local neighborhood (the target hexagon)

d = the width of local sample window (the target hexagon and its first- and second-order neighbors)

x_j = the value of neighbor j

w_{ij} = the weight of neighbor j from location i (all the neighboring hexagons in the moving window were given an equal weight of 1)

n = number of samples in the dataset (the 9,644 hexagons containing tree cover)

W_i^* = the sum of the weights

$s_1^* i$ = the number of samples within d of the central location (19: the focal hexagon and its 18 first- and second-order neighbors)

$\bar{x}^*$ = the mean of whole dataset (in this case, for all 9,644 hexagons containing tree cover)

s^* = the standard deviation of whole dataset (for all 9,644 hexagons containing tree cover)

G_i^* is standardized as a z-score with a mean of 0 and a standard deviation of 1, with values >1.96 representing significant local clustering of higher fire occurrence densities (p <0.025) and values <-1.96 representing significant clustering of lower fire occurrence densities (p <0.025), because 95 percent of the observations under a normal distribution should be within approximately two standard deviations of the mean (Laffan 2006). Values between -1.96 and 1.96 have no statistically significant concentration of high or low values; a hexagon and its 18 neighbors, in other words, have a normal range of both high and low numbers of fire occurrences per 100 km^2 of tree canopy cover area. It is worth noting that the threshold values are not exact because the correlation of spatial data violates the assumption of independence required for statistical significance (Laffan 2006). In addition, the Getis-Ord approach does not require that the input data be normally distributed, because the local G_i^* values are computed under a randomization assumption, with G_i^* equating to a standardized z-score that asymptotically tends to a normal distribution (Anselin 1992). The z-scores are considered to be reliable, even with skewed data, as long as the local neighborhood encompasses several observations (ESRI 2015), in this case, via the target hexagon and its 18 first- and second-order neighbors.

RESULTS AND DISCUSSION

Trends in Forest Fire Occurrence Detections for 2018

The MODIS Active Fire database recorded 76,692 forest fire occurrences across the conterminous United States in 2018, the ninth most in 18 full years of data collection (fig. 3.1). This was approximately 24 percent less than in 2017 (100,840 total forest fire occurrences), and nearly identical to the annual mean of 76,165 forest fire occurrences across the previous 17 years of data collection. In Alaska, meanwhile, the MODIS database encompassed 690 forest fire occurrences in 2018, about 67 percent fewer than the preceding year (2,064) and about 93 percent fewer than the previous 17-year annual mean of 9,340. Meanwhile, Hawaii had 136 fire occurrences in 2018, an increase of about 216 percent from the previous year (43) but 57 percent below the average of 317 fire occurrences over the previous 17 years. Finally, a single forest fire occurrence was detected in Puerto Rico, 89 percent fewer than the previous average of about 9 per year.

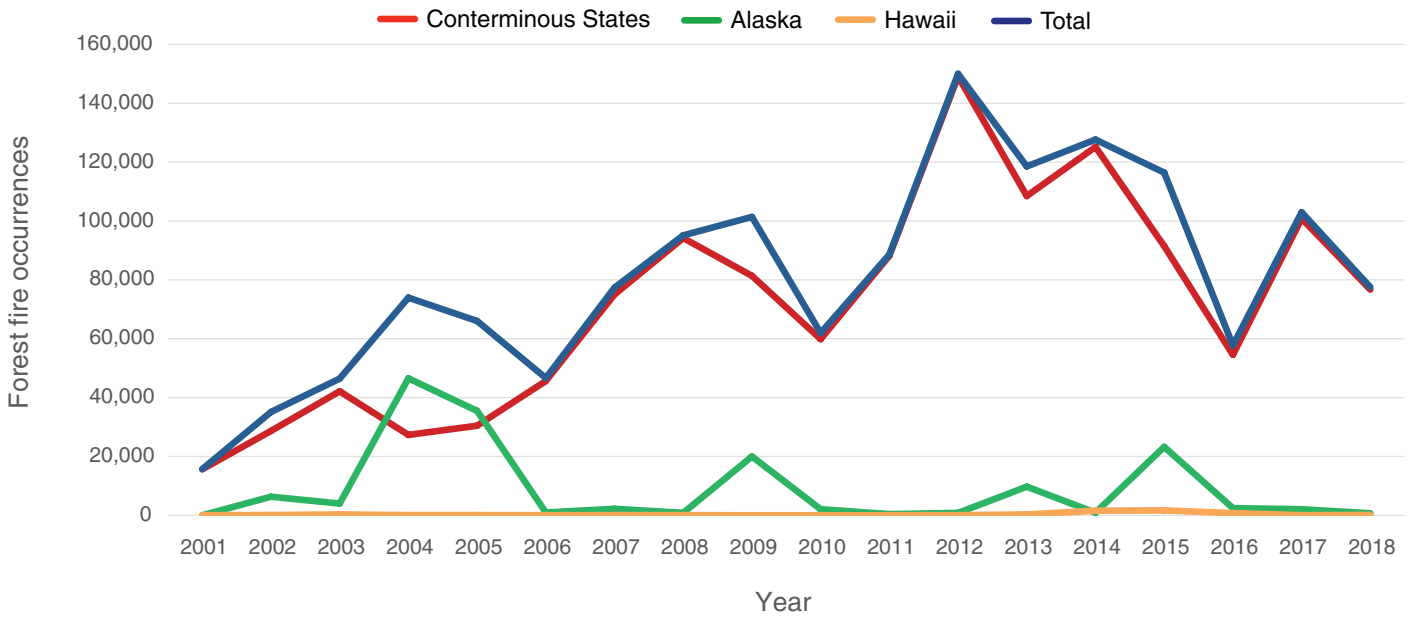

Figure 3.1—Forest fire occurrences detected by MODIS from 2001 to 2018 for the conterminous United States, Alaska, and Hawaii, and for the entire Nation combined. (Data source: U.S. Department of Agriculture Forest Service, Geospatial Technology and Applications Center, in conjunction with the NASA MODIS Rapid Response group)

The decrease in the total number of fire occurrences across the United States derived from MODIS is generally consistent with the official wildland fire statistics, which are based on other data sources and reported a below-normal number of wildfires (National Interagency Coordination Center 2019). In 2018, 58,083 wildland fires were reported across the United States, which was a decrease from 71,499 in 2017. The area burned nationally (3 548 078 ha) was 87 percent of the 2017 burned area total (4 057 413 ha) but 132 percent of the 10-year average (National Interagency Coordination Center 2018, 2019). The number of wildland fires and fire complexes exceeding 16 187 ha (a benchmark threshold for the National Interagency Coordination Center) was 49 in 2018, compared to 44 in 2017 and 19 in 2016 (National Interagency Coordination Center 2017, 2018). As noted in the Methods section, estimates of burned area are different metrics for quantifying fire activity than calculations of MODIS-detected fire occurrences, though the two may be correlated.

Areas with the highest fire occurrence densities in 2018 were in northern California and in north-central Washington (fig. 3.2). Beginning in July, these areas experienced drier-than-normal conditions which expanded

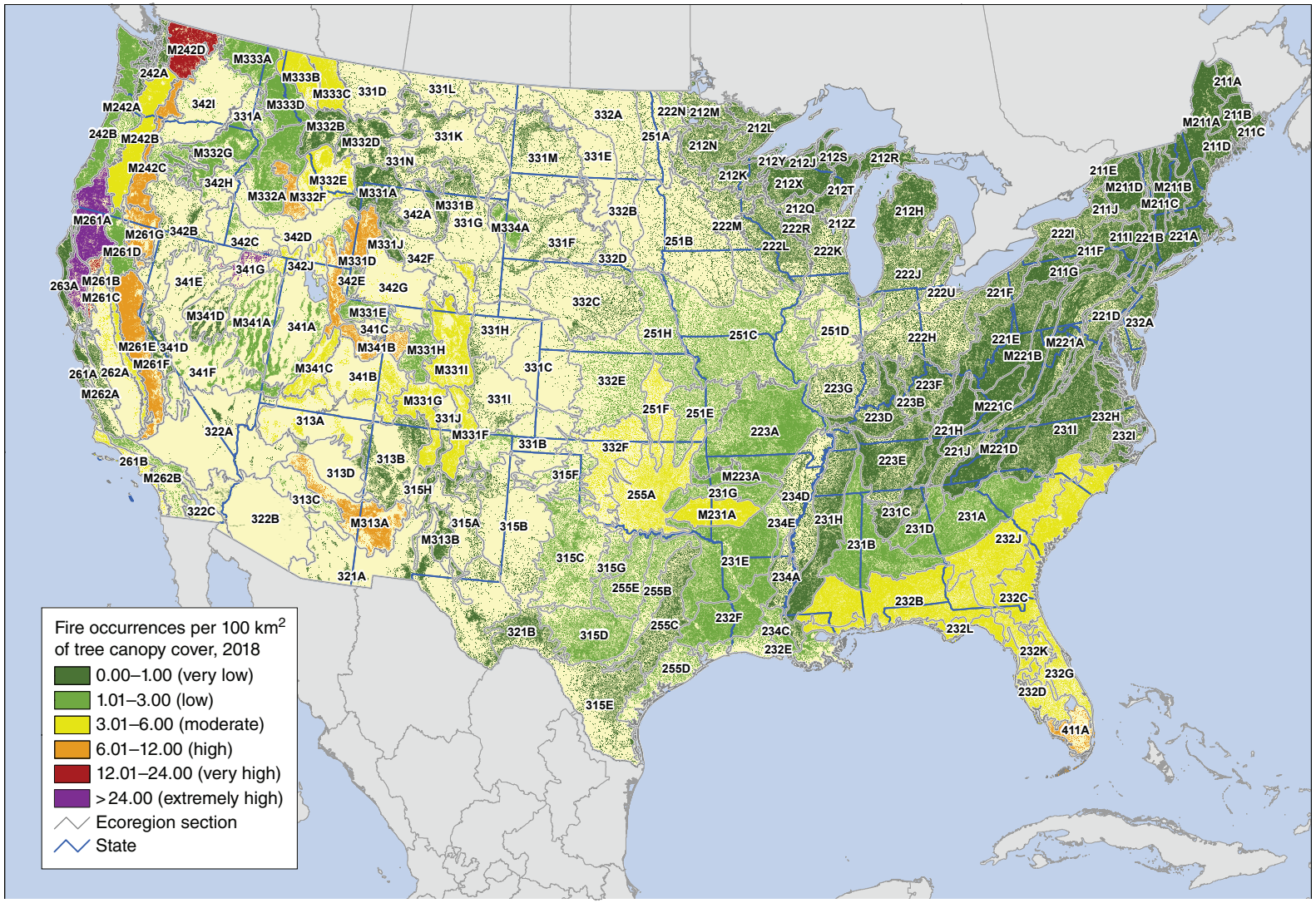

Figure 3.2—The number of forest fire occurrences, per 100 km^2 (10 000 ha) of tree canopy coverage area, by ecoregion section within the conterminous 48 States, for 2018. The gray lines delineate ecoregion sections (Cleland and others 2007). Tree canopy cover is based on data from a cooperative project between the Multi-Resolution Land Characteristics Consortium (Coulston and others 2012) and the Forest Service Geospatial Technology and Applications Center using the 2011 National Land Cover Database. (Source of fire data: U.S. Department of Agriculture Forest Service, Geospatial Technology and Applications Center, in conjunction with the NASA MODIS Rapid Response group)

and intensified through the autumn months, resulting in fuels that were critically dry (National Interagency Coordination Center 2019). The ecoregion section with the highest fire occurrence density was the Northern California Coast Ranges (M261B), which experienced 31.8 fire occurrences/100 km^2 of tree canopy cover (table 3.1) and included the Mendocino Fire Complex, which was the largest recorded fire complex in California history (CAL FIRE 2019), burning 185 800 ha between July 27 and September 18 and costing approximately $220 million for containment (National Interagency Coordination Center 2019). In the neighboring M261A–Klamath Mountains ecoregion section of northern California and southwestern Oregon, fire occurrence densities were also extremely high (29.0 fire occurrences/100 km^2 of tree canopy cover). This ecoregion was the location of the Carr Fire, which burned 92 936 ha in California, killed eight people, and cost approximately $162 million (CAL FIRE 2019, National Interagency Coordination Center 2019), and of

Table 3.1—The 15 ecoregion sections in the conterminous United States with the highest fire occurrence densities in 2018

Section	Name	Tree canopy area	Fire occurrences	Density
		km^2	*number*	*fire occurrences per 100 km^2 of tree canopy coverage area*
M261B	Northern California Coast Ranges	114.1	3,630	31.8
341G	Northeastern Great Basin	24.6	754	30.6
M261A	Klamath Mountains	338.5	9,818	29.0
M261C	Northern California Interior Coast Ranges	18.2	283	15.5
M242D	Northern Cascades	251.1	3,838	15.3
M261E	Sierra Nevada	427.8	4,863	11.4
M261G	Modoc Plateau	128.7	1,427	11.1
411A	Everglades	68.7	630	9.2
M331D	Overthrust Mountains	262.2	2,147	8.2
M313A	White Mountains-San Francisco Peaks-Mogollon Rim	202.5	1,622	8.0
M332F	Challis Volcanics	72.2	547	7.6
M341B	Tavaputs Plateau	92.0	670	7.3
M242C	Eastern Cascades	219.4	1,549	7.1
M333B	Flathead Valley	168.9	1,013	6.0
262A	Great Valley	19.4	114	5.9

the Klondike and Taylor Creek Fires in Oregon, which scorched 70 924 ha and 21 383 ha, respectively.

Three other ecoregion sections in northern California also had high fire occurrence densities: M261C–Northern California Interior Coast Ranges (15.5 fire occurrences/100 km^2 of tree canopy cover), M261E–Sierra Nevada (11.4 fire occurrences/100 km^2 of tree canopy cover), and M261G–Modoc Plateau (11.1 fire occurrences/100 km^2 of tree canopy cover) (fig. 3.2). M261E–Sierra Nevada was the location of the Camp Fire. This fire burned 62 053 ha between November 8 and 25, consumed the town of Paradise, CA, and killed 85 people, making it the deadliest U.S. fire in more than a century (National Interagency Coordination Center 2019).

In northeastern Nevada, 341G–Northeastern Great Basin, an area with relatively sparse tree canopy cover, had an extremely high 30.6 fire occurrences/100 km^2 of canopy cover as a result of the 176 269-ha Martin Fire, which burned in July and was the largest fire in the State's history (National Interagency Coordination Center 2019, Rothberg 2018). Meanwhile, the fire occurrence density in M242D–Northern Cascades (15.3 fire occurrences/100 km^2) in north-central Washington was also high, in part because of the Crescent Mountain Fire, which burned 22 909 ha between July and November, and the Cougar Creek Fire, which burned 17 285 ha during the same period (National Interagency Coordination Center 2019).

High fire occurrence densities (6.01–12.00 fire occurrences/100 km^2 of tree canopy cover) were recorded in a handful of other western ecoregion sections: M331D–Overthrust Mountains, in western Wyoming, southeastern Idaho, and northern Utah; M313A–White Mountains-San Francisco Peaks-Mogollon Rim, in east-central Arizona and west-central New Mexico; M332F–Challis Volcanics in central Idaho; M341B–Tavaputs Plateau, in northeastern Utah and northwestern Colorado; and M242C–Eastern Cascades, in central Washington and Oregon (table 3.1). Only one ecoregion in the Eastern United States had a high fire occurrence density in 2018, 411A–Everglades (9.2) (fig. 3.2).

Higher-than-usual temperatures throughout the year in Alaska, meanwhile, were combined with consistently above-average precipitation throughout the State (National Interagency Coordination Center 2019). As a result, fire occurrence densities across the State were low, which no ecoregions exceeding 1 fire occurrence/100 km^2 of forest and shrub cover (fig. 3.3).

In Hawaii, the dramatic Big Island eruption of lava through 24 new fissures in the lower east rift zone of the Kīlauea volcano burned forests and consumed 700 homes at the very eastern tip of the island (Andrews 2018), resulting in a fire occurrence density of 7.4/100 km^2 of tree canopy cover in the island's Lowland Wet-Hilo-Puna ecoregion (LWh-hp) (fig. 3.4). The eruption also affected the neighboring Mesic ecoregion (MEh), where fire occurrence density was 3.2/100 km^2 of tree canopy cover. All other

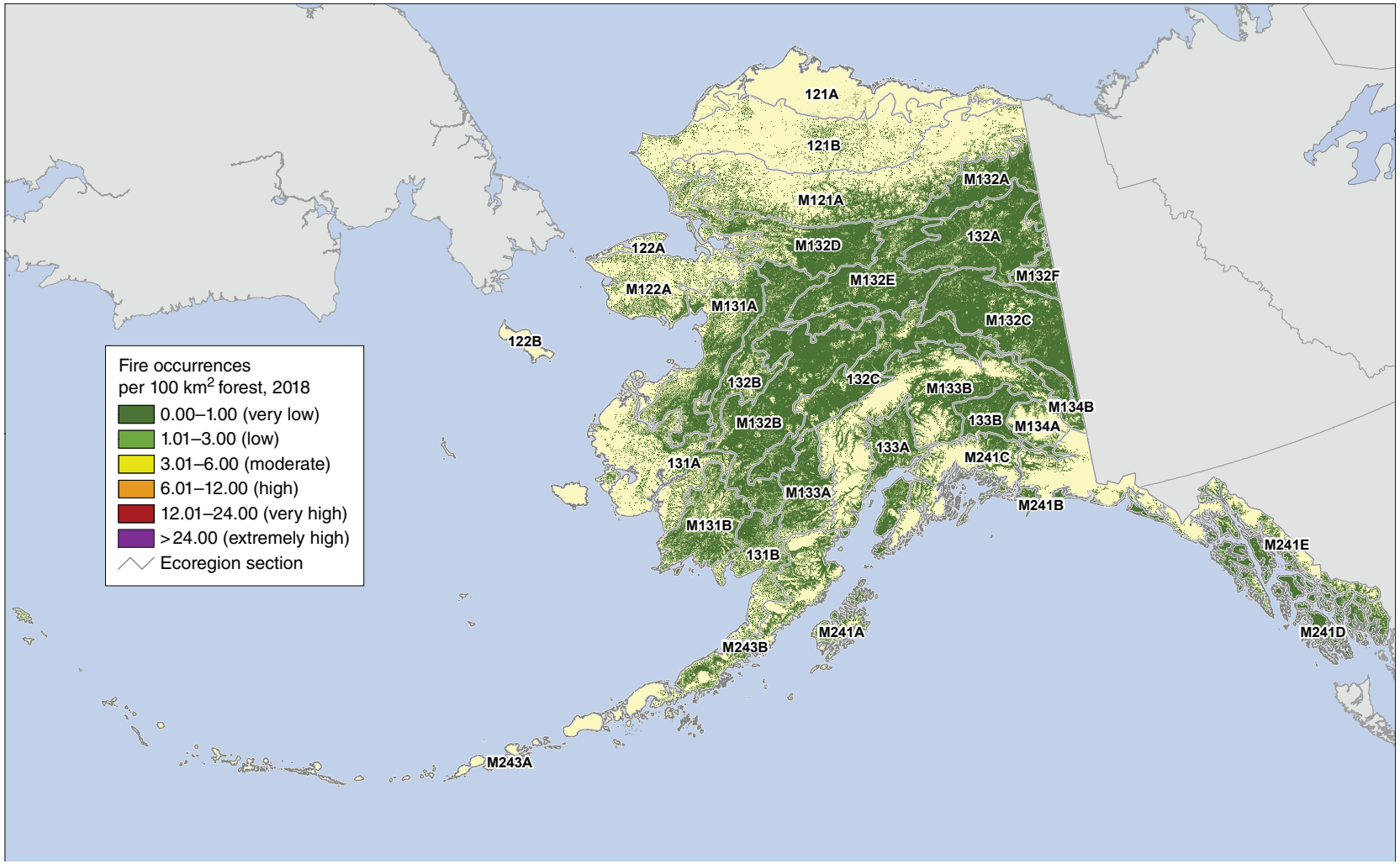

Figure 3.3—The number of forest fire occurrences, per 100 km^2 (10 000 ha) of forest and shrub cover, by ecoregion section within Alaska, for 2018. The gray lines delineate ecoregion sections (Spencer and others 2002). Forest and shrub cover is derived from the 2011 National Land Cover Database. (Source of fire data: U.S. Department of Agriculture Forest Service, Geospatial Technology and Applications Center, in conjunction with the NASA MODIS Rapid Response group)

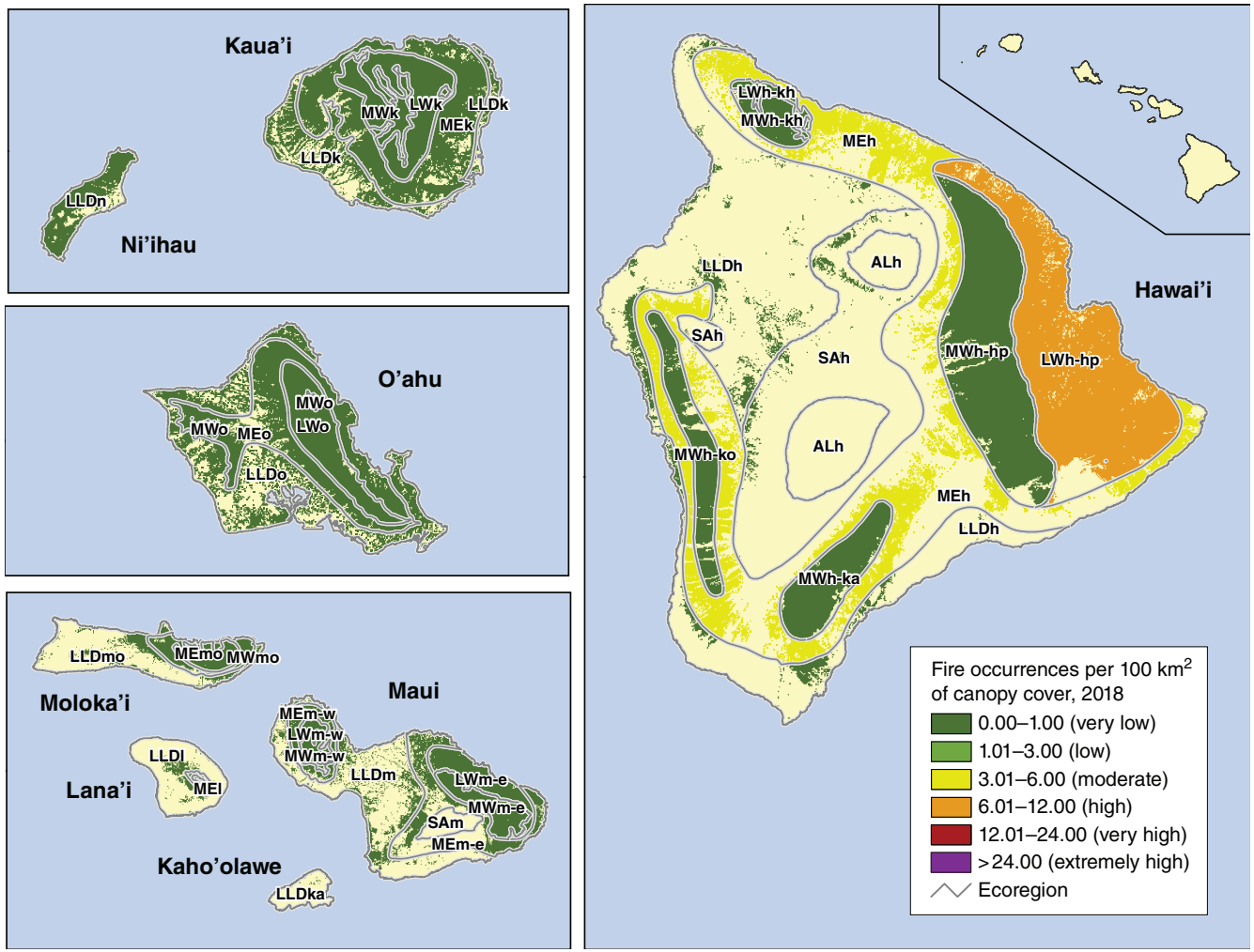

Figure 3.4—The number of forest fire occurrences, per 100 km^2 (10 000 ha) of tree canopy coverage area, by island/ecoregion combination in Hawaii, for 2018. Tree canopy cover is based on data from a cooperative project between the Multi-Resolution Land Characteristics Consortium (Coulston and others 2012) and the Forest Service Geospatial Technology and Applications Center using the 2011 National Land Cover Database. See figure 1.2 for ecoregion identification. (Source of fire data: U.S. Department of Agriculture Forest Service, Geospatial Technology and Applications Center, in conjunction with the NASA MODIS Rapid Response group)

ecoregions in the State had fire occurrence densities of ≤1 fire occurrence/100 km^2 of tree canopy cover.

Finally, fire occurrence densities were all ≤1 fire occurrence/100 km^2 of tree canopy cover for all of the islands constituting the U.S. Caribbean territories (Puerto Rico and the U.S. Virgin Islands) in 2018 (fig. 3.5).

Comparison to Longer Term Trends

The nature of the MODIS Active Fire data makes it possible to contrast, for each ecoregion in the conterminous States, Alaska, and Hawaii, and for each Caribbean island, short-term (2018) forest fire occurrence densities with longer term trends encompassing the first 17 full years of data collection (2001–2017). In general, the ecoregion sections of the conterminous States with the highest annual fire occurrence means are located in the northern Rocky Mountains, California, the Southwest, and the Southeastern Coastal Plain, while most ecoregion sections within the Northeastern, Midwestern, Middle Atlantic, and Appalachian regions experienced ≤3 fire occurrences/100 km^2 of tree canopy cover annually during the multiyear period (fig. 3.6A). The forested ecoregion section that experienced the most annual fire occurrences on average was M332A–Idaho Batholith in central Idaho (mean annual fire occurrence density of 13.4) (table 3.2). Other ecoregion sections with high mean fire occurrence densities (6.01–12.00 fire occurrences/100 km^2 of canopy cover) were located along the Gulf Coast in the Southeast; in coastal, northern, and central areas of California; in north-central Washington; in central Arizona and New Mexico; in the northern Rocky Mountains; and in central Kansas and northeastern Oklahoma (table 3.2). The ecoregion section with the greatest variation in fire occurrence densities from 2001 to 2017 was M332A–Idaho Batholith, with more moderate variation in California, northern Washington, southern and northeastern Oregon, western Montana, and central Arizona and west-central New Mexico (fig. 3.6B). Less variation occurred throughout the central Rocky Mountain States, the Great Basin, the Southeast, and central Oregon and Washington. The lowest levels of variation occurred throughout most of the Midwest and Northeast.

As determined by the calculation of standardized fire occurrence *z*-scores, ecoregion sections in northern California; northeastern Nevada; the central Rocky Mountains of southeastern Idaho, southwestern Wyoming, northeastern Utah, northwestern and south-central Colorado, and northeastern New Mexico; and southern Florida experienced significantly greater fire occurrence densities than normal in 2018, compared to the previous 17-year mean and accounting for variability over time (fig. 3.6C). The ecoregion section with the highest *z*-score in 2018 was 341G–Northeastern Great Basin, location of the Martin Fire. Additionally, some ecoregion sections in the West had moderately or slightly higher fire occurrence density than expected as indicated by their *z*-scores (fig. 3.6C), including M261A–Klamath Mountains in northern California

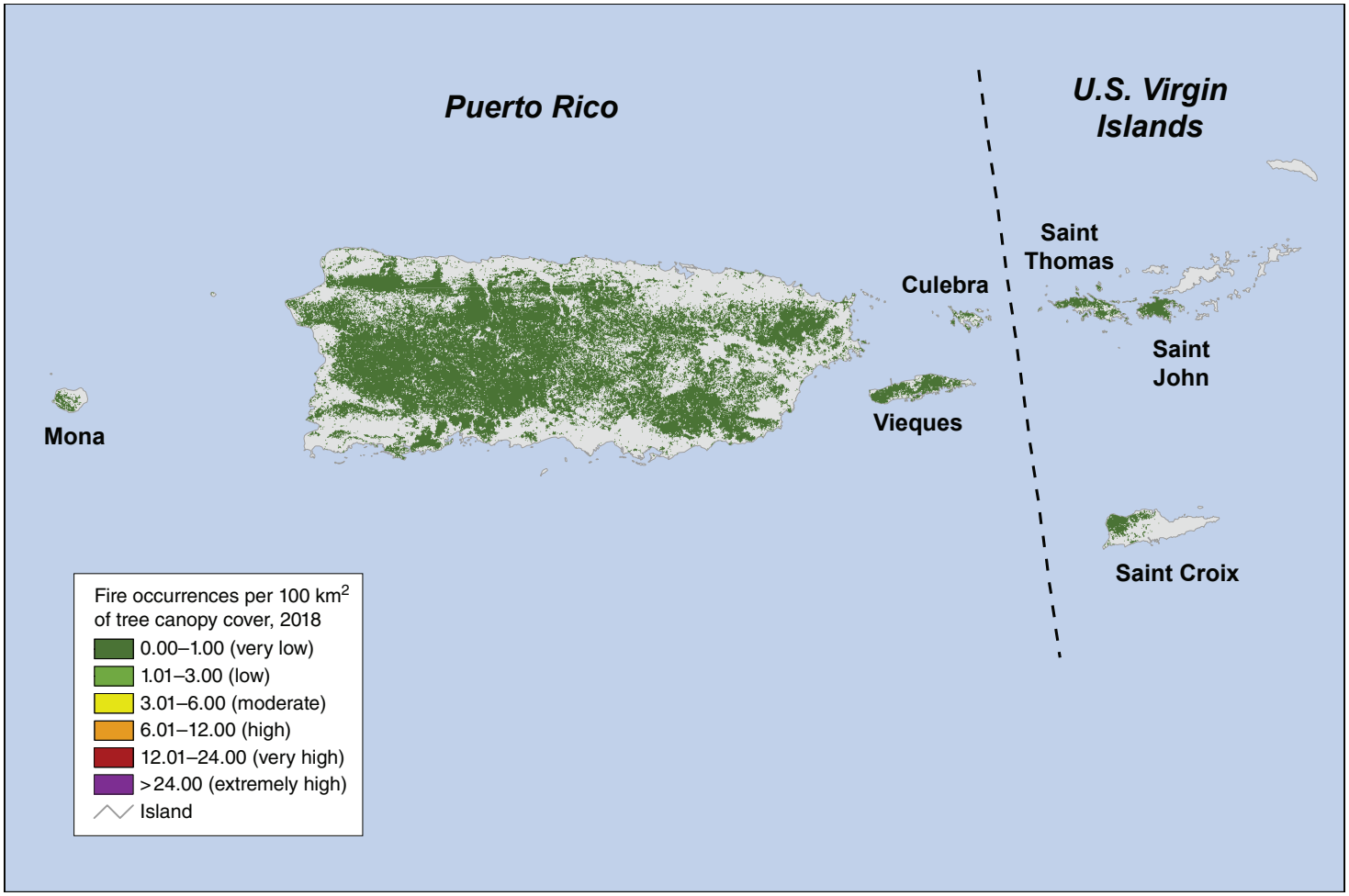

Figure 3.5—The number of forest fire occurrences, per 100 km^2 (10 000 ha) of tree canopy coverage area, by island in Puerto Rico and the U.S. Virgin Islands, for 2018. Tree canopy cover is based on data from a cooperative project between the Multi-Resolution Land Characteristics Consortium (Coulston and others 2012) and the Forest Service Geospatial Technology and Applications Center using the 2011 National Land Cover Database. (Source of fire data: U.S. Department of Agriculture Forest Service, Geospatial Technology and Applications Center, in conjunction with the NASA MODIS Rapid Response group)

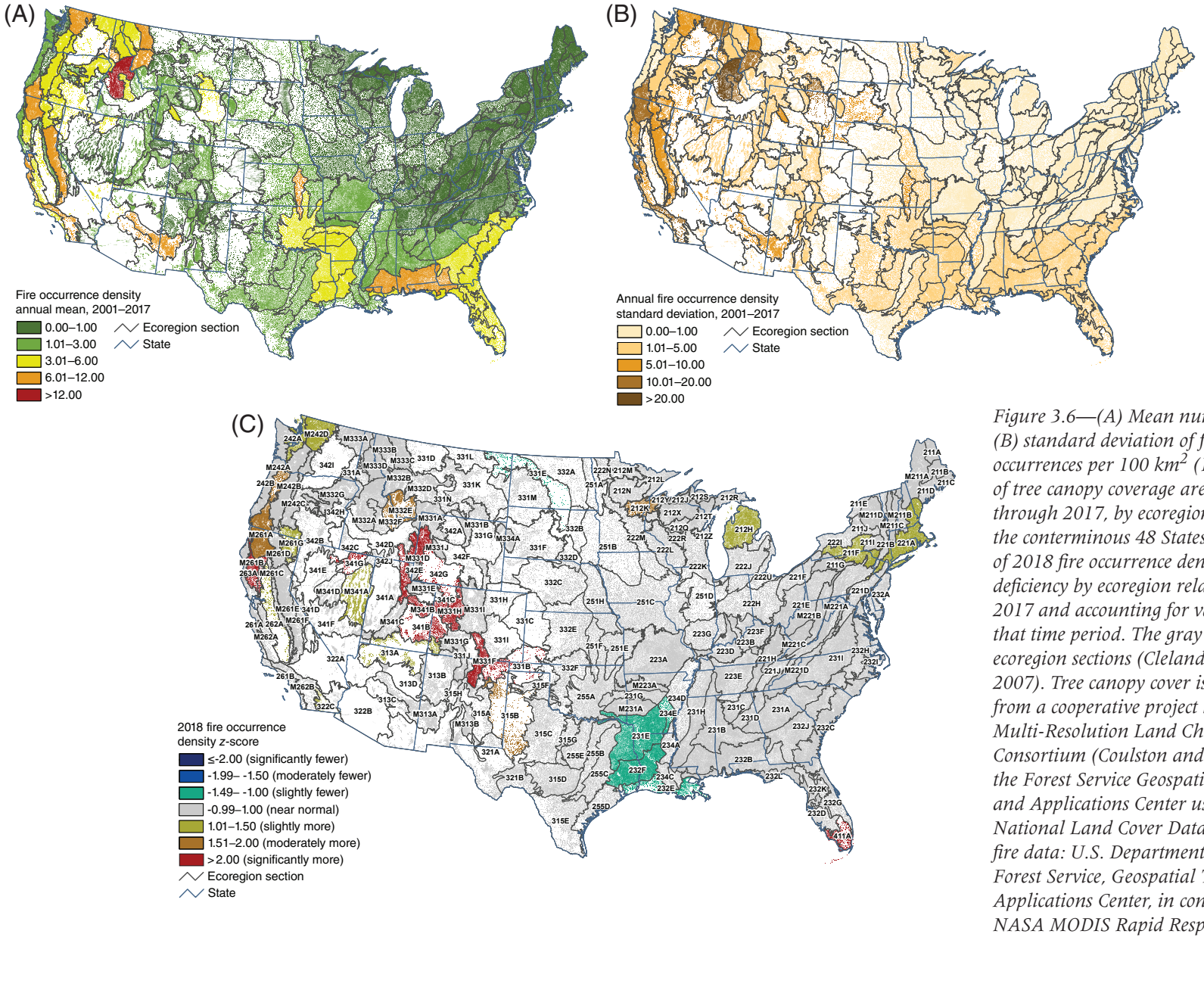

Figure 3.6—(A) Mean number and (B) standard deviation of forest fire occurrences per 100 km^2 (10 000 ha) of tree canopy coverage area from 2001 through 2017, by ecoregion section within the conterminous 48 States. (C) Degree of 2018 fire occurrence density excess or deficiency by ecoregion relative to 2001–2017 and accounting for variation over that time period. The gray lines delineate ecoregion sections (Cleland and others 2007). Tree canopy cover is based on data from a cooperative project between the Multi-Resolution Land Characteristics Consortium (Coulston and others 2012) and the Forest Service Geospatial Technology and Applications Center using the 2011 National Land Cover Database. (Source of fire data: U.S. Department of Agriculture Forest Service, Geospatial Technology and Applications Center, in conjunction with the NASA MODIS Rapid Response group)

Table 3.2—The 15 ecoregion sections in the conterminous United States with the highest annual mean fire occurrence densities from 2001 through 2017

Section	Name	Tree canopy area	Mean annual fire occurrence density
		km^2	*fire occurrences per 100 km^2 of tree canopy coverage area*
M332A	Idaho Batholith	338.9	13.4
M261A	Klamath Mountains	338.5	9.6
M262B	Southern California Mountain and Valley	58.1	9.2
313C	Tonto Transition	17.5	7.8
M261E	Sierra Nevada	427.8	7.7
M313A	White Mountains-San Francisco Peaks-Mogollon Rim	202.5	7.7
251F	Flint Hills	57.8	7.1
261A	Central California Coast	66.8	6.7
M242D	Northern Cascades	251.1	6.1
232B	Gulf Coastal Plains and Flatwoods	888.7	6.1
331A	Palouse Prairie	33.4	6.0
M332B	Northern Rockies and Bitterroot Valley	154.9	6.0
M333C	Northern Rockies	176.3	6.0
M332F	Challis Volcanics	72.2	6.0
232J	Southern Atlantic Coastal Plains and Flatwoods	604.0	5.3

and southwestern Oregon, 242B–Willamette Valley in northwestern Oregon, and M332E–Beaverhead Mountains in east-central Idaho and southwestern Montana. A number of ecoregions in the Midwest and Northeast also experienced slightly or moderately more fire occurrences than normal: 212K–Western Superior Uplands in west-central Minnesota and northwest Wisconsin, 212H–Northern Lower Peninsula in Michigan, 211F–Northern Glaciated Allegheny Plateau in southern New York and northern Pennsylvania, and 221A–Lower New England.

A handful of ecoregion sections in the south-central part of the country, meanwhile, had lower fire occurrence densities in 2018 compared to the longer term as indicated by their *z*-scores: 231E–Mid Coastal Plains-Western in eastern Texas, southwestern Arkansas, and southeastern Oklahoma; 234E–Arkansas Alluvial Plains in southeastern Arkansas; 232F–Coastal Plains and

Flatwoods-Western Gulf in southeastern Texas and central Louisiana; and 232E–Louisiana Coastal Prairie and Marshes in southern Louisiana (fig. 3.6C). Each of these had a very low fire occurrence density score in 2018, with some having somewhat higher annual mean fire occurrence densities for 2001–2017.

In Alaska, meanwhile, moderate mean fire occurrence density existed in the east-central and central parts of the State, encompassing 132A–Yukon-Old Crow Basin and M132E–Ray Mountains (fig. 3.7A). These same areas, along with M132C–Yukon-Tanana Uplands and M132F–North Ogilvie Mountains, experienced the greatest degree of variability over the 17-year period preceding 2018 (fig. 3.7B). In 2018, no ecoregion sections were outside the range of near-normal fire occurrence density (z-score ≤-1 or >1) for the previous 17 years and accounting for variability (fig. 3.7C).

In Hawaii, both mean annual fire occurrence density (fig. 3.8A) and variability (fig. 3.8B) were highest in the Lowland Wet-Hilo-Puna ecoregion (LWh-hp) of the Big Island during the 2001–2017 period. The annual mean was ≤1 fire occurrence/100 km^2 of tree cover for all other ecoregions except the Mesic region on the Big Island (MEh), which was 2.2. In 2018, only one Hawaiian island/ecoregion combination was outside the range of near-normal fire occurrence density, controlling for variability over the previous 17 years (z-score ≤-1 or >1). This was the Lowland/Leeward Dry ecoregion on Maui (LLDm), which had slightly fewer fire occurrences than expected (fig. 3.7C).

All the islands of the Caribbean territories had annual fire occurrence means and standard deviations ≤1 (figs. 3.9A and 3.9B). Among the Caribbean islands, only Puerto Rico was outside the range of near-normal fire occurrence density (z-score ≤-1 or >1) in 2018, having slightly fewer fire occurrences than expected (fig. 3.9C).

Geographical Hot Spots of Fire Occurrence Density

Although summarizing fire occurrence data at the ecoregion section scale allows for the quantification of fire occurrence density across the country, a geographical hot spot analysis can offer insights into where, statistically, fire occurrences are more concentrated than expected by chance. In 2018, the SASH method detected one geographic hot spot of extremely high fire occurrence density (G_i^* >24) and four hot spots of very high fire occurrence density (G_i^* >12 and ≤24) (fig. 3.10). The hot spot of extremely high density was in northern California, in ecoregion sections M261B–Northern California Coast Ranges and M261C–Northern California Interior Coast Ranges. Three of the four hot spots of very high occurrence density were also in northern California and southwestern Oregon, contained within ecoregions shown by earlier analysis to be locations of high fire occurrence density (fig. 3.2). The fourth hot spot was in north-central Washington (M242D–Northern Cascades).

Hot spots of high fire occurrence density (G_i^* >6 and ≤12) were identified in south-central Oregon (M242C–Eastern Cascades and

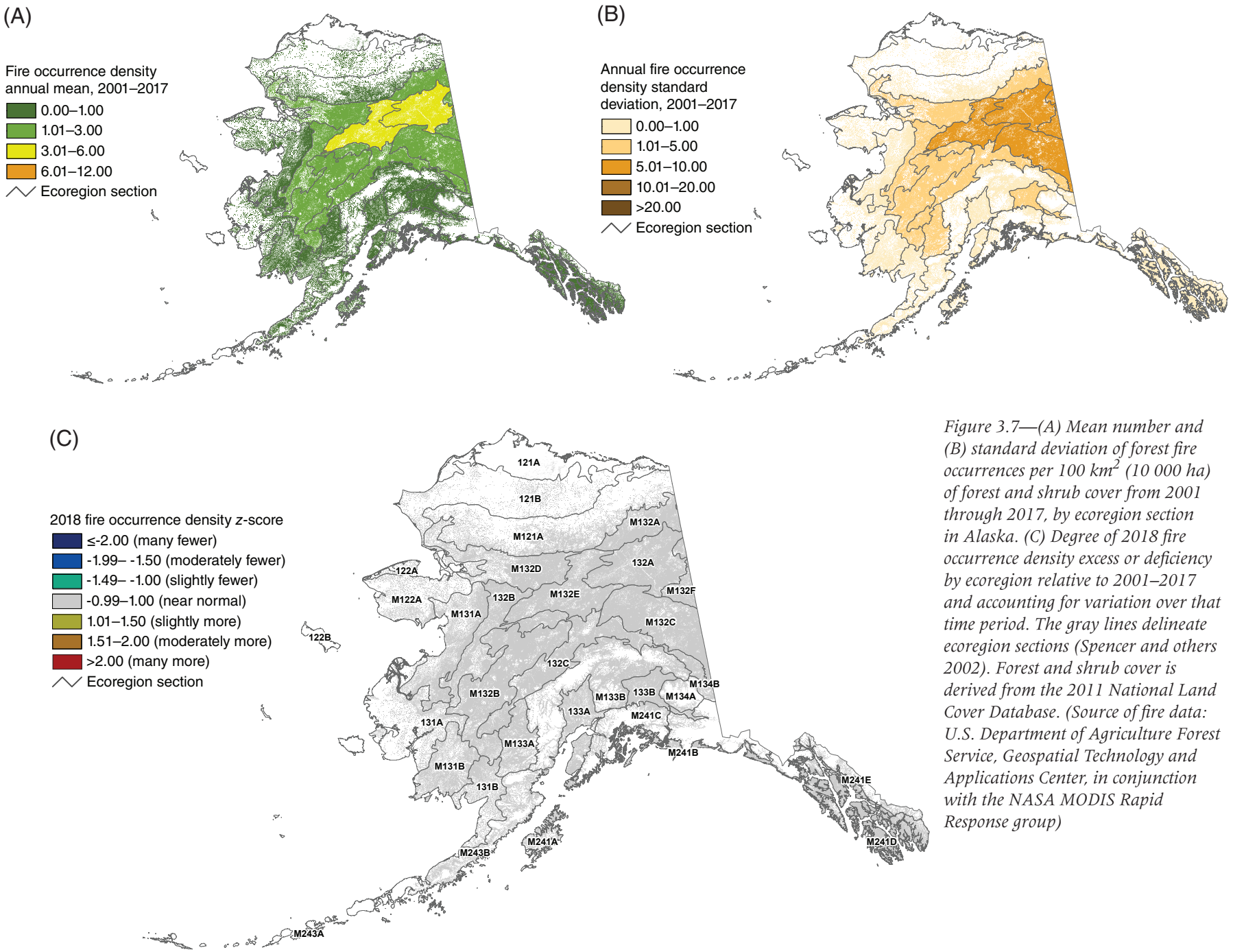

Figure 3.7—(A) Mean number and (B) standard deviation of forest fire occurrences per 100 km^2 (10 000 ha) of forest and shrub cover from 2001 through 2017, by ecoregion section in Alaska. (C) Degree of 2018 fire occurrence density excess or deficiency by ecoregion relative to 2001–2017 and accounting for variation over that time period. The gray lines delineate ecoregion sections (Spencer and others 2002). Forest and shrub cover is derived from the 2011 National Land Cover Database. (Source of fire data: U.S. Department of Agriculture Forest Service, Geospatial Technology and Applications Center, in conjunction with the NASA MODIS Rapid Response group)

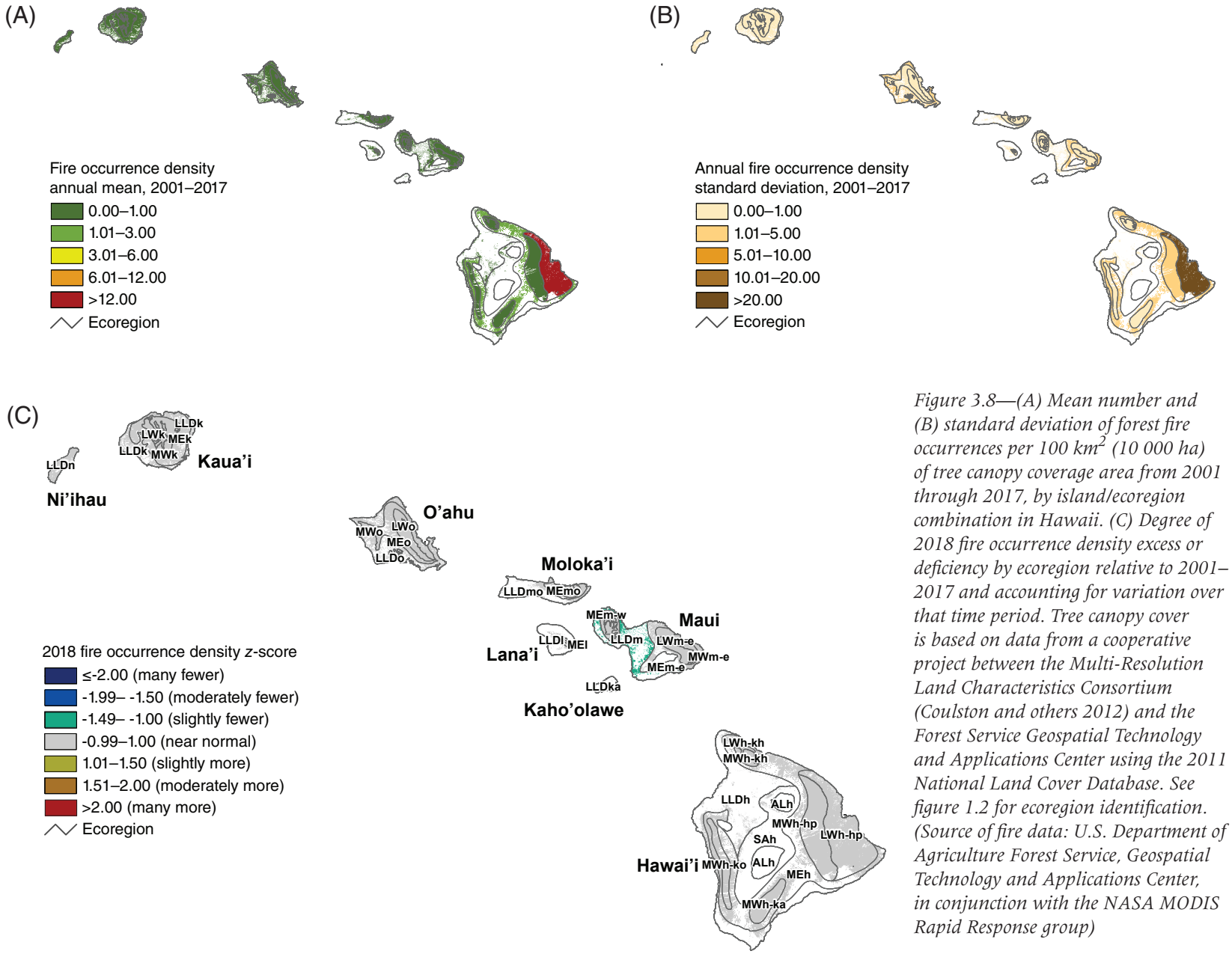

Figure 3.8—(A) Mean number and (B) standard deviation of forest fire occurrences per 100 km^2 (10 000 ha) of tree canopy coverage area from 2001 through 2017, by island/ecoregion combination in Hawaii. (C) Degree of 2018 fire occurrence density excess or deficiency by ecoregion relative to 2001–2017 and accounting for variation over that time period. Tree canopy cover is based on data from a cooperative project between the Multi-Resolution Land Characteristics Consortium (Coulston and others 2012) and the Forest Service Geospatial Technology and Applications Center using the 2011 National Land Cover Database. See figure 1.2 for ecoregion identification. (Source of fire data: U.S. Department of Agriculture Forest Service, Geospatial Technology and Applications Center, in conjunction with the NASA MODIS Rapid Response group)

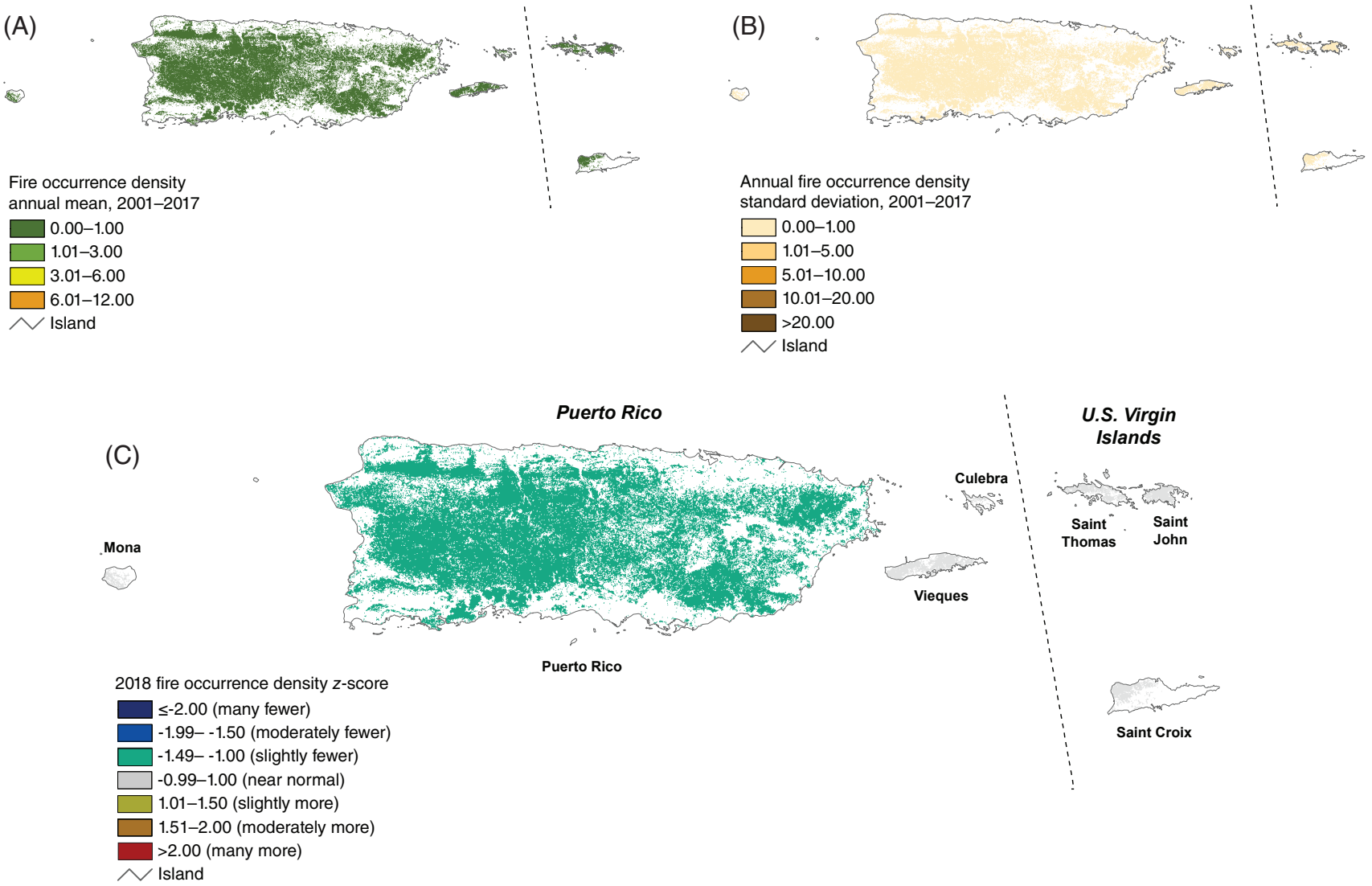

Figure 3.9—(A) Mean number and (B) standard deviation of forest fire occurrences per 100 km^2 (10 000 ha) of forested area from 2001 through 2017, by island in Puerto Rico and the U.S. Virgin Islands. (C) Degree of 2018 fire occurrence density excess or deficiency by ecoregion relative to 2001–2017 and accounting for variation over that time period. Tree canopy cover is based on data from a cooperative project between the Multi-Resolution Land Characteristics Consortium (Coulston and others 2012) and the U.S. Department of Agriculture Forest Service, Geospatial Technology and Applications Center using the 2011 National Land Cover Database.

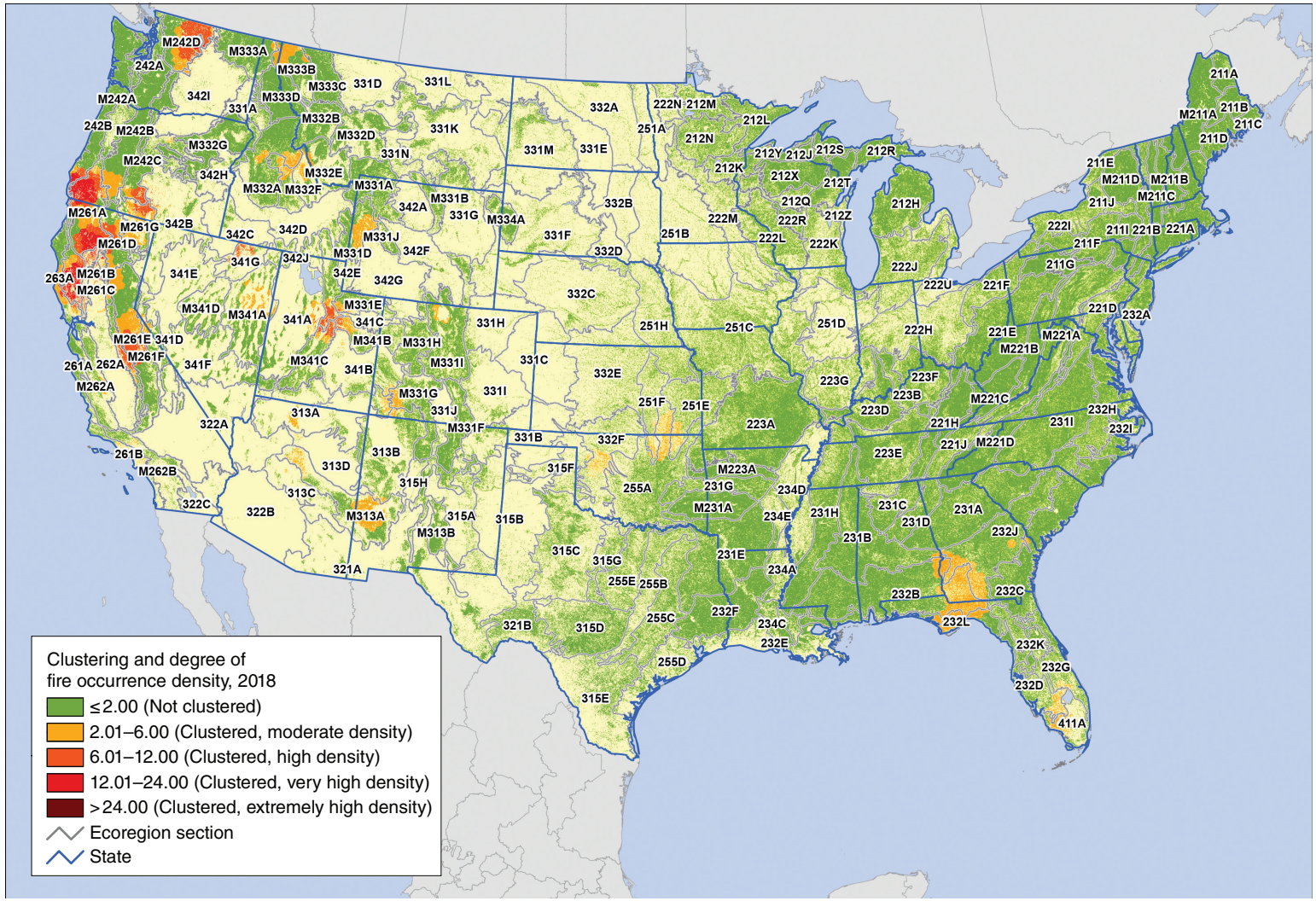

Figure 3.10—Hot spots of fire occurrence across the conterminous United States for 2018. Values are Getis-Ord Gi* *scores, with values >2 representing significant clustering of high fire occurrence densities. (No areas of significant clustering of lower fire occurrence densities, <-2, were detected). The gray lines delineate ecoregion sections (Cleland and others 2007). Background tree canopy cover is based on data from a cooperative project between the Multi-Resolution Land Characteristics Consortium (Coulston and others 2012) and the Forest Service Geospatial Technology and Applications Center using the 2011 National Land Cover Database. (Source of fire data: U.S. Department of Agriculture Forest Service, Geospatial Technology and Applications Center, in conjunction with the NASA MODIS Rapid Response group)*

M261G–Modoc Plateau), the Sierra Nevada of California (M261E), northeastern Nevada (341G–Northeastern Great Basin), and central Utah (M331D–Overthrust Mountains, M331E–Uinta Mountains, M341B–Tavaputs Plateau, and M341C–Utah High Plateau).

Hot spots of moderate fire density in 2018 (G_i^* >2 and ≤6) were identified in scattered locations within the Rocky Mountain States, the southern Plains States, and the Southeast (fig. 3.10). From west to east, these were detected in:

- Northwestern Montana and northern Idaho (M333B–Flathead Valley)
- Central Idaho (M332A–Idaho Batholith, M332E–Beaverhead Mountains, and M332F–Challis Volcanics)
- Eastern Nevada (M341A–East Great Basin and Mountains)
- Northern Arizona (313A–Grand Canyon)
- Central Arizona (M313A–White Mountains-San Francisco Peaks-Mogollon Rim)
- Western Wyoming (M331D–Overthrust Mountains)
- Southwestern New Mexico (M313A–White Mountains-San Francisco Peaks-Mogollon Rim)
- Southwestern Colorado (M331G–South Central Highlands and 313B–Navajo Canyonlands)
- North-central Colorado (M331I–Northern Parks and Ranges)
- West-central Oklahoma (332F–South Central and Red Bed Plains)
- Southeastern Kansas and northeastern Oklahoma (251F–Flint Hills, 255A–Cross Timbers and Prairie, and 251E–Osage Plains)
- Florida Panhandle and southwestern Georgia (232B–Gulf Coastal Plains and Flatwoods, 232J–Southern Atlantic Coastal Plains and Flatwoods, and 232L–Gulf Coastal Lowlands)
- Southern Florida (232D– Florida Coastal Lowlands-Gulf and 411A–Everglades)

CONCLUSIONS AND FUTURE WORK

In 2018, the number of MODIS satellite-detected forest fire occurrences recorded for the conterminous States was the ninth most in 18 full years of data collection and was nearly identical to the annual mean of forest fire occurrences across the previous 17 years of data collection. Ecoregion sections in northern California/southwestern Oregon, north-central Washington, and northeastern Nevada had the highest forest fire occurrence density per 100 km^2 of tree canopy cover area. Geographic hot spots of high fire occurrence density were detected in these same areas, as well as in Utah and the Sierra Nevada of California. Ecoregion sections in northern California; the Cascade Mountains of Oregon and Washington; northern and eastern Nevada; the central Rocky Mountains; central Minnesota; northern Michigan; and the Northeastern States experienced greater fire occurrence density than normal compared to the previous 17-year mean and accounting for variability over time.

Ecoregions in eastern Texas, southern Arkansas, and much of Louisiana, meanwhile, had lower fire occurrence density than expected. Alaska had low fire occurrence densities throughout the State. In Hawaii, the Lowland Wet ecoregion of the Big Island experienced relatively high fire occurrence density because of a volcanic eruption near the eastern tip of the island.

The results of these geographic analyses are intended to offer insights into where fire occurrences have been concentrated spatially in a given year and compared to previous years but are not intended to quantify the severity of a given fire season. Given the limits of MODIS active fire detection using 1-km resolution data, these products also may underrepresent the number of fire occurrences in some ecosystems where small and low-intensity fires are common, and where high cloud frequency can interfere with fire detection. These products can also have commission errors. However, these high-temporal-fidelity products currently offer the best means for daily monitoring of forest fire occurrences.

Future work related to understanding geographic patterns of forest fire occurrences in the United States could include a comparison of the MODIS detections with those of the VIIRS sensor, an analysis of fire occurrence detections by forest cover types, an evaluation of whether the fire occurrences correspond with mapped burned areas, an assessment of the relationships between fire occurrence and drought conditions, and an analysis of the potential ecological consequences of high fire occurrence densities using data such as those available from the Forest Inventory and Analysis program.

Ecological and forest health impacts relating to fire and other abiotic disturbances are scale-dependent properties, which in turn are affected by management objectives (Lundquist and others 2011). Information about the concentration of fire occurrences may help pinpoint areas of concern for aiding management activities and for investigations into the ecological and socioeconomic impacts of forest fire potentially outside the range of historic frequency.

LITERATURE CITED

Andrews, R.G. 2018. America's most hazardous volcano erupted this year. Then it erupted and erupted. The New York Times. December 12. https://www.nytimes.com/2018/12/12/science/kilauea-hawaii-volcano-eruption.html. [Date accessed: July 15, 2019].

Anselin, L. 1992. Spatial data analysis with GIS: an introduction to application in the social sciences. Technical Report 92-10. Santa Barbara, CA: University of California, National Center for Geographic Information and Analysis. 53 p.

Barbour, M.G.; Burk, J.H.; Pitts, W.D. [and others]. 1999. Terrestrial plant ecology. Menlo Park, CA: Addison Wesley Longman, Inc. 649 p.

Bond, W.J.; Keeley, J.E. 2005. Fire as a global "herbivore": the ecology and evolution of flammable ecosystems. Trends in Ecology & Evolution. 20(7): 387–394.

CAL FIRE. 2019. Top 20 largest California wildfires. https://fire.ca.gov/media/5510/top20_acres.pdf. [Date accessed: July 15, 2019].

Cleland, D.T.; Freeouf, J.A.; Keys, J.E. [and others]. 2007. Ecological subregions: sections and subsections for the conterminous United States. Gen. Tech. Rep. WO-76D. Washington, DC: U.S. Department of Agriculture Forest Service. Map; Sloan, A.M., cartographer; presentation scale 1:3,500,000; colored. Also on CD-ROM as a GIS coverage in ArcINFO format or at http://data.fs.usda.gov/geodata/edw/datasets.php. [Date accessed: July 20, 2015].

Coulston, J.W.; Moisen, G.G.; Wilson, B.T. [and others]. 2012. Modeling percent tree canopy cover: a pilot study. Photogrammetric Engineering and Remote Sensing. 78(7): 715–727.

Coulston, J.W.; Ambrose, M.J.; Riitters, K.H.; Conkling, B.L. 2005. Forest Health Monitoring 2004 national technical report. Gen. Tech. Rep. SRS-90. Asheville, NC: U.S. Department of Agriculture Forest Service, Southern Research Station. 81 p.

Edmonds, R.L.; Agee, J.K.; Gara, R.I. 2011. Forest health and protection. Long Grove, IL: Waveland Press, Inc. 667 p.

ESRI. 2015. ArcMap® 10.3. Redlands, CA: Environmental Systems Research Institute.

Getis, A.; Ord, J.K. 1992. The analysis of spatial association by use of distance statistics. Geographical Analysis. 24(3): 189–206.

Gill, A.M.; Stephens, S.L.; Cary, G.J. 2013. The worldwide "wildfire" problem. Ecological Applications. 23(2): 438–454.

Hawbaker, T.J.; Radeloff, V.C.; Syphard, A.D. [and others]. 2008. Detection rates of the MODIS active fire product. Remote Sensing of Environment. 112: 2656–2664.

Homer, C.G.; Dewitz, J.A.; Yang, L. [and others]. 2015. Completion of the 2011 National Land Cover Database for the conterminous United States: representing a decade of land cover change information. Photogrammetric Engineering and Remote Sensing. 81(5): 345–354.

Justice, C.O.; Giglio, L.; Korontzi, S. [and others]. 2002. The MODIS fire products. Remote Sensing of Environment. 83(1–2): 244–262.

Justice, C.O.; Giglio, L.; Roy, D. [and others]. 2011. MODIS-derived global fire products. In: Ramachandran, B.; Justice, C.O.; Abrams, M.J., eds. Land remote sensing and global environmental change: NASA's earth observing system and the science of ASTER and MODIS. New York: Springer: 661–679.

Laffan, S.W. 2006. Assessing regional scale weed distributions, with an Australian example using *Nassella trichotoma*. Weed Research. 46(3): 194–206.

Lundquist, J.E.; Camp, A.E.; Tyrrell, M.L. [and others]. 2011. Earth, wind and fire: abiotic factors and the impacts of global environmental change on forest health. In: Castello, J.D.; Teale, S.A., eds. Forest health: an integrated perspective. New York: Cambridge University Press: 195–243.

McKenzie, D.; Peterson, D.L.; Alvarado, E. 1996. Predicting the effect of fire on large-scale vegetation patterns in North America. Res. Pap. PNW-489. Portland, OR: U.S. Department of Agriculture Forest Service, Pacific Northwest Research Station. 38 p.

National Interagency Coordination Center. 2017. Wildland fire summary and statistics annual report: 2016. http://www.predictiveservices.nifc.gov/intelligence/2016_Statssumm/intro_summary16.pdf. [Date accessed: May 30, 2017].

National Interagency Coordination Center. 2018. Wildland fire summary and statistics annual report: 2017. https://www.predictiveservices.nifc.gov/intelligence/2017_statssumm/intro_summary17.pdf. [Date accessed: April 30, 2018].

National Interagency Coordination Center. 2019. Wildland fire summary and statistics annual report: 2018. https://www.predictiveservices.nifc.gov/intelligence/2018_statssumm/intro_summary18.pdf. [Date accessed: June 27, 2019].

Nowacki, G.J.; Abrams, M.D. 2008. The demise of fire and "mesophication" of forests in the Eastern United States. BioScience. 58(2): 123–138.

Potter, K.M. 2012a. Large-scale patterns of forest fire occurrence in the conterminous United States and Alaska, 2005–07. In: Potter, K.M.; Conkling, B.L., eds. Forest Health Monitoring 2008 national technical report. Gen. Tech. Rep. SRS-158. Asheville, NC: U.S. Department of Agriculture Forest Service, Southern Research Station: 73–83.

Potter, K.M. 2012b. Large-scale patterns of forest fire occurrence in the conterminous United States and Alaska, 2001–08. In: Potter, K.M.; Conkling, B.L., eds. Forest Health Monitoring 2009 national technical report. Gen. Tech. Rep. SRS-167. Asheville, NC: U.S. Department of Agriculture Forest Service, Southern Research Station: 151–161.

Potter, K.M. 2013a. Large-scale patterns of forest fire occurrence in the conterminous United States and Alaska, 2009. In: Potter, K.M.; Conkling, B.L., eds. Forest Health Monitoring: national status, trends, and analysis 2010. Gen. Tech. Rep. SRS-176. Asheville, NC: U.S. Department of Agriculture Forest Service, Southern Research Station: 31–39.

Potter, K.M. 2013b. Large-scale patterns of forest fire occurrence in the conterminous United States and Alaska, 2010. In: Potter, K.M.; Conkling, B.L., eds. Forest Health Monitoring: national status, trends, and analysis 2011. Gen. Tech. Rep. SRS-185. Asheville, NC: U.S. Department of Agriculture Forest Service, Southern Research Station: 29–40.

Potter, K.M. 2014. Large-scale patterns of forest fire occurrence in the conterminous United States and Alaska, 2011. In: Potter, K.M.; Conkling, B.L., eds. Forest Health Monitoring: national status, trends, and analysis 2012. Gen. Tech. Rep. SRS-198. Asheville, NC: U.S. Department of Agriculture Forest Service, Southern Research Station: 35–48.

Potter, K.M. 2015a. Large-scale patterns of forest fire occurrence in the conterminous United States and Alaska, 2012. In: Potter, K.M.; Conkling, B.L., eds. Forest Health Monitoring: national status, trends, and analysis 2013. Gen. Tech. Rep. SRS-207. Asheville, NC: U.S. Department of Agriculture Forest Service, Southern Research Station: 37–53.

Potter, K.M. 2015b. Large-scale patterns of forest fire occurrence in the conterminous United States and Alaska, 2013. In: Potter, K.M.; Conkling, B.L., eds. Forest Health Monitoring: national status, trends, and analysis 2014. Gen. Tech. Rep. SRS-209. Asheville, NC: U.S. Department of Agriculture Forest Service, Southern Research Station: 39–55.

Potter, K.M. 2016. Large-scale patterns of forest fire occurrence in the conterminous United States, Alaska, and Hawaii, 2014. In: Potter, K.M.; Conkling, B.L., eds. Forest Health Monitoring: national status, trends, and analysis 2015. Gen. Tech. Rep. SRS-213. Asheville, NC: U.S. Department of Agriculture Forest Service, Southern Research Station: 41–60.

Potter, K.M. 2017. Large-scale patterns of forest fire occurrence in the conterminous United States, Alaska, and Hawaii, 2015. In: Potter, K.M.; Conkling, B.L., eds. Forest Health Monitoring: national status, trends, and analysis 2016. Gen. Tech. Rep. SRS-222. Asheville, NC: U.S. Department of Agriculture Forest Service, Southern Research Station: 43–62.

Potter, K.M. 2018. Large-scale patterns of forest fire occurrence in the conterminous United States, Alaska, and Hawaii, 2016. In: Potter, K.M.; Conkling, B.L., eds. Forest Health Monitoring: national status, trends, and analysis 2017. Gen. Tech. Rep. SRS-233. Asheville, NC: U.S. Department of Agriculture Forest Service, Southern Research Station: 45–64.

Potter, K.M. 2019. Large-scale patterns of forest fire occurrence across the 50 United States and the Caribbean territories, 2017. In: Potter, K.M.; Conkling, B.L., eds. Forest Health Monitoring: national status, trends, and analysis 2018. Gen. Tech. Rep. SRS-239. Asheville, NC: U.S. Department of Agriculture Forest Service, Southern Research Station: 51–76.

Potter, K.M.; Koch, F.H.; Oswalt, C.M.; Iannone, B.V. 2016. Data, data everywhere: detecting spatial patterns in fine-scale ecological information collected across a continent. Landscape Ecology. 31: 67–84.

Pyne, S.J. 2010. America's fires: a historical context for policy and practice. Durham, NC: Forest History Society. 91 p.

Reams, G.A.; Smith, W.D.; Hansen, M.H. [and others]. 2005. The Forest Inventory and Analysis sampling frame. In: Bechtold, W.A.; Patterson, P.L., eds. The enhanced Forest Inventory and Analysis program—national sampling design and estimation procedures. Asheville, NC: U.S. Department of Agriculture Forest Service, Southern Research Station: 11–26.

Richardson, L.A.; Champ, P.A.; Loomis, J.B. 2012. The hidden cost of wildfires: economic valuation of health effects of wildfire smoke exposure in southern California. Journal of Forest Economics. 18(1): 14–35.

Rothberg, D. 2018. 'It's gone, it's gone': Nation's largest wildfire in Nevada devastates ranches, sage grouse. The Nevada Independent. July 12. https://thenevadaindependent.com/article/its-gone-its-gone-nations-largest-wildfire-in-nevada-devastates-ranches-sage-grouse. [Date accessed: July 15, 2019].

Schmidt, K.M.; Menakis, J.P.; Hardy, C.C. [and others]. 2002. Development of coarse-scale spatial data for wildland fire and fuel management. Gen. Tech. Rep. RMRS-87. Fort Collins, CO: U.S. Department of Agriculture Forest Service, Rocky Mountain Research Station. 41 p.

Shima, T.; Sugimoto, S.; Okutomi, M. 2010. Comparison of image alignment on hexagonal and square lattices. In: 2010 IEEE international conference on image processing. [Place of publication unknown]: Institute of Electrical and Electronics Engineers, Inc.: 141–144. DOI: 10.1109/icip.2010.5654351.

Spencer, P.; Nowacki, G.; Fleming, M. [and others]. 2002. Home is where the habitat is: an ecosystem foundation for wildlife distribution and behavior. Arctic Research of the United States. 16: 6–17.

Tonini, M.; Tuia, D.; Ratle, F. 2009. Detection of clusters using space-time scan statistics. International Journal of Wildland Fire. 18(7): 830–836.

U.S. Department of Agriculture (USDA) Forest Service. 2008. National forest type data development. http://svinetfc4.fs.fed.us/rastergateway/forest_type/. [Date accessed: May 13, 2008].

U.S. Department of Agriculture (USDA) Forest Service. 2019. MODIS active fire mapping program: fire detection GIS data. https://fsapps.nwcg.gov/afm/gisdata.php. [Date accessed: May 7, 2019].

White, D.; Kimerling, A.J.; Overton, W.S. 1992. Cartographic and geometric components of a global sampling design for environmental monitoring. Cartography and Geographic Information Systems. 19(1): 5–22.